New Journal and we have not received input yet 21 (2021) 100778

Contents lists available at ScienceDirect

Thermal Science and Engineering Progress

journal homepage: www.sciencedirect.com/journal/thermal-science-and-engineering-progress

Investigate the technical-economical feasibility of utilizing the available industrial waste thermal energy in Oman

Abdullah Al-Janabi *, Ghassan Al-Hajri, Tariq Al-Maashani

Department of Mechanical & Industrial Engineering, College of Engineering, Sultan Qaboos University, P.O. Box: 33, P.C. 123 Alkhoud, Muscat, Oman

ARTICLE INFO

Keywords:
Heat recovery
Waste thermal energy
Organic Rankine cycle
Thermal performance

ABSTRACT

The rapid increasing in energy demand is starting to create a burden on Oman due to its unrenewable sources of energy. Oman is formulating policies to promote using renewable energy technologies and/or minimize energy losses in industrial sectors through using waste heat recovery techniques. In this study, waste thermal energy data of five industrial companies were used to evaluate the performance of an Organic Rankine Cycle (ORC) unit. It has been found that the ORC technology might become a technically feasible solution to enhance the performance of industrial thermal cycles in Oman by converting the available waste thermal energy into an additional electric power. The level of enhancement is found to be affected (directly proportional relationship) by the range of temperature and mass flow rate of the available thermal source. With respect to environment effect, high performance was achieved at the first and the last quarters of the year where water coolant temperature is low during winter seasons, while the performance deteriorated is summer as result of high water coolant temperature. Unfortunately, using ORC at Sharq Sohar Steel Rolling Mills is inapplicable, i.e. the required parasitic load was greater than the work output of the expander. The economic feasibility calculations showed that using ORC unit at ACWA Power Barka I would be an economically feasible project in terms of payback period of approximately 6 years and revenue percentage of 85%. In contrast, the available waste heat at Areej Vegetable Oil & Derivatives cannot be economically recovered to electric power as a result of its long time-span of payback period.

1. Introduction

It is not only in Oman but in all parts of the world that mechanical and electric energies are in such great demand. Thermal energy is still the most popular means of generating mechanical and electric energy. Fossil fuels are one of the main sources of obtaining thermal power which is applicable to many thermodynamic cycles. Such examples are: internal combustion engines, gas turbines, steam turbines, etc. These processes and machines have one main thing in common which is, they use a high temperature heat source and generally don't achieve a cycle efficiency of more than 55% [1]. Consequently, a lot of waste of thermal energy is being released in these cycles. According to American Department of Energy (DOE), it has been concluded that between 20 and 50% of industrial energy input is lost as waste thermal energy in terms of cooling water and hot exhaust gases [2]. One of the methods for minimizing industrial thermal energy losses is to carry out energy saving programs which focus on reducing energy demands and improving energy efficiency within industrial and domestic areas. Other methods include improving the efficiency of the cycles in order to reduce the amount of thermal energy wasted within their processes. An energy system can be improved by utilizing heat that would otherwise go to waste. In up-to-date plants, the maximum enhancement in thermal efficiency can be achieved by as much as 20% or more [3]. There are a number of methods which can be applied in order to improve energy cycles efficiency such as: Enhancing and optimizing components within the cycle is one of the conventional methods that are used to achieve higher levels of efficiency. Using heat recovery heat exchangers is a great method of reducing cost by reducing fuel consumption in many facilities, through re-entering the waste heat into the cycle in order to preheat the working fluid before entering a boiler, evaporator, etc. This process is called heat recovery for waste heat-to-heat applications and it has a wide range of applicability, regardless of industry type [4,5]. The problem with the previous methods is that industrial waste thermal energy cannot always be reused on-site or for local areas. In addition, most of the industrial companies are not interested to invest heat recovery projects of payback period of more than three years [2]. In addition to that, the heat recovery isn't feasible or possible in certain

* Corresponding author.
E-mail address: ab.aljanabi@squ.edu.om (A. Al-Janabi).

https://doi.org/10.1016/j.tsep.2020.100778
Received 5 May 2020; Received in revised form 2 September 2020; Accepted 8 November 2020
Available online 24 November 2020

Nomenclatures

CO_2	Carbon dioxide [–]
C_p	Specific heat [kJ/kg. °C]
EBITDA	Earnings Before Interest, Taxes, Depreciation, and Amortization
GWP	Global Warming Potential [–]
GHG	Greenhouse Gas [–]
h	Enthalpy [kJ/kg]
M	Dimensionless mass flow rate [–]
$\dot{m}$	Mass flow rate [kg/s]
ODP	Ozone Depletion Potential [–]
ORC	Organic Rankine Cycle [–]
PBP	Payback period [year]
P_{low}	Low pressure [kPa]
P_{high}	High pressure [kPa]
$\dot{Q}_{in}$	Input heat [kW]
R-245fa	Hydrofluorocarbon [–]
s	Entropy [kJ/kg. K]
T	Temperature [K]
W	Work [kJ/kg]
$\dot{W}_{net}$	Net power output [kW]
x	quality [–]

Greek

η_{th}	Thermal efficiency [%]
η_{rev}	Reversible thermal efficiency [%]

Subscripts

cs	cooling source
exp	expander
evap	evaporator
hs	heat source
i	inlet
ref	refrigerant
s	isentropic
th	thermal
rev	reversible

instances, and the existing technical and non-technical barriers play a decisive role in deaccelerating the wide-spread implementation of the heat recovery techniques such as lack of regulations and policies.

Another alternative solution for dealing with the waste thermal energy is the utilization of the available waste heat source as an energy source which can be either converted into mechanical or electrical power. There are many applications where low-grade waste thermal energy has been effectively recovered for use in industrial facilities. The success of recovering the low-grade waste thermal energy is, in fact, due to the development in Organic Rankine Cycle (ORC) technology [6]. Organic Rankine Cycle is a proven commercially available technology to convert waste thermal energy which would otherwise be dissipated into the atmosphere into power. It has been found that ORC-projects with renewable energy applications were overall found to be very attractive [1]. Wei et al. [7], found that maximizing the use of exhaust heat by ORC system was a good way to improve the system net power output. From the economical point of view, the ORC projects are not always profitable. The investment cost is mainly determined by the size of the module, integration cost, complexity, generated electricity profit and government support. For example, Low temperature ORC's become available from about 1350 €/kWe for a 250 kW-unit to 2200 €/kWe for 50 kW-units. Turbine based ORC's (high temperature) range from 1000 €/kWe for a 2 MW-unit, to 2000 €/kWe for a 500 kW-unit and up to 3000 €/kWe for a 150 kW-unit. These are all average prices based only on the ORC module prices. Installation costs are very variable and are strongly site and application dependent. For waste heat recovery applications, these can range from 50% (higher power range) to 100% (lower power range) of the ORC module's cost [1].

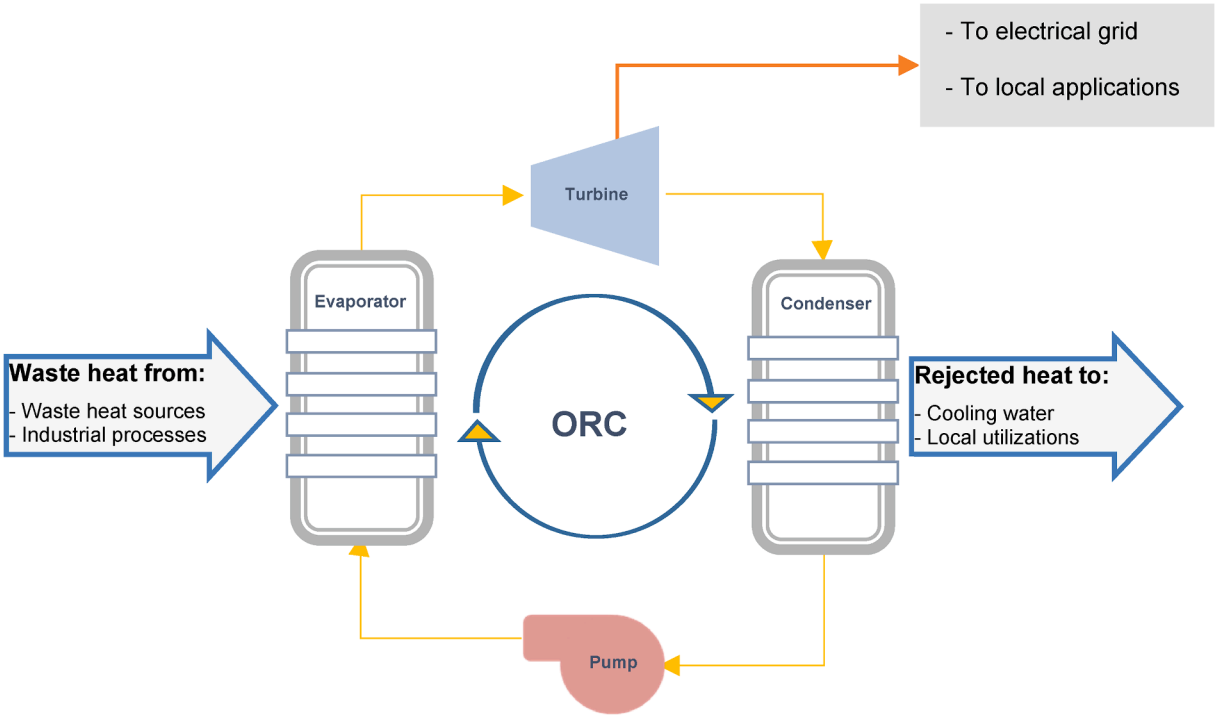

Fig. 1. Organic Rankine Cycle unit components.

Table 1
Industrial waste heat source data in Muscat-Oman.

Location	Company	Heat source type	Flow rate ($\dot{m}$)	Specific heat capacity (C_p)	Inlet (waste heat) temperature (T_1)	Outlet (waste heat) temperature (T_2)	Available thermal energy (Q_{th})
		-	kg/s	kJ/ kg. °C	°C	°C	kW
Rusayl	Areej vegetable oils & derivatives	Water	0.975	4.181	80	*50	122.29
Sohar	Sharq Sohar Steel Rolling Mills	Water	6.945	4.181	60	**40	580.7
Barka	ACWA Power Barka I	Water	4.69	4.181	105	*85	392.2
Ghubra	Al Ghubra Power & Desalination	Water	4.394	4.181	115	*95	367.43
Rusayl	Al Rusail Power Plant	Lube oil	18.3	2.131	80	*60	779.95

* The outlet temperatures are estimated values based on the size of the ORC evaporator.
** The outlet temperatures given by the industry.

Energy sources in Oman are mainly depended on the production of fossil fuels and natural gas., where most plants and industries rely on them to power the stations and plants [8]. In line with Oman's aspirations and Oman vision 2040, reducing fuel consumption to eliminate the dependency on less-environment-friendly fossil fuels becomes an essential target. To achieve such a target, it is required to use an effective alternative energy source and/or minimize the energy losses in industrial sectors through the utilization of the waste thermal energy. Due to the lake of scientific work and results on ORC application in Oman, this study endeavors to evaluate the performance of utilization the ORC technology for converting the available industrial waste thermal energy in Oman into electrical power. This might lead to; i) provide more power to the electrical grid or be directly supplied to local applications, ii) develop a reduction in fuel consumption that is directly reflected on the economic saving potential, iii) reduce the emitted CO_2 which could provide an additional benefit to the environmental considerations. In addition, the power required to cool the waste heat in the main cycle will be heavily reduced by using the ORC technology.

2. ORC work principles and design concept

The Organic Rankine Cycle generally consists of the six main components: (1) evaporator, (2) condenser, (3) expander, (4) pump, (5) generator and (6) the working fluid as shown in Fig. 1. The thermodynamic principle of the ORC follows the same principle of the traditional steam Rankine cycle, with one main difference, which is the working fluid. In other words, water is the working fluid of Rankine cycle that demands a lot of heat to vaporize, thus a lot of thermal energy is required making industrial waste heat unsuitable [9,10], while organic fluids with a lower evaporation heat requirement are used as an alternative working fluid in the ORC for recovering the waste thermal energy such as R-134a, R-245fa, R-1234yf, etc. Organic fluids (refrigerants) require an evaporation heat value about 10 times less than water, these results in higher mass flows in the ORC-cycle, and so much bigger feed pumps are needed compared with a steam cycle [1,9,10]. In addition, Organic fluids have a 10 times higher molar weight or density, and therefore require smaller turbine diameters. Despite the main difference between an ORC and a steam power cycle is related to the utilized working fluid, it is essential to shed light on the major differences with respect to their operating principle. The organic fluids have the ability to recover heat sources of low range temperature as a result of their low boiling temperature, which in turn develop less thermal stresses on turbine/expander blades. Such behavior would not be the case of using water. In addition, most of organic fluids are having condenser pressure higher than the atmospheric pressure which could prevent the cycle from air infiltrations, while this is not the case for water's condensing pressure. It should be noted that, the consumed power associated with ORC's pumps is higher than that of steam cycle pumps. This is, in fact, due to the lower pressure difference and higher volumetric flow rate of the organic fluids. The considerable disadvantages of organic fluids are mainly linked to their characteristics, e.g. some of them are flammable, toxic not environmentally-friendly, and are cost effective as water. Perhaps the most important difference between the two cycles is their efficiencies with the ORC rarely reaching a maximum of 24% and a typical steam Rankine Cycle with more than 30% which make steam Rankine Cycles more efficient than ORC cycles [11].

Designing an ORC unit and selecting suitable, efficient components for building-up the unit is strongly dependent on the waste thermal energy source operating conditions, which in fact varies from place to place. Add to that, working conditions of the cycle and thermodynamic properties of the working fluids have a tremendous impact on performance of the ORC system, environmental impact and economic viability [12,13]. As a preliminary step for designing the ORC unit, the industrial data related to the available waste heat sources for 5 local Omani companies have been collected as listed in Table 1. Such limited number of the selected companies for this study is, in fact, related to the conservative behavior for some companies with respect to share their industrial data for research projects, especially for the mixed private-public ownership companies and private ownership companies. However, the selected companies cover the range of middle and large industrial sector in Oman and will provide a deep insight of the available energy saving potential in this country. The data than analyzed and used

Table 2
Design parameters of the ORC unit.

Item	heat source type (water)	waste heat mass flow rate	temperature gradient across the heat source	evaporating temperature T_{evap} [1]	Heat source temperature $T_{hs,in}$ [2]	Heat sinks temperature [3]	Pinch points [4]	cooling system [5]
Design variables		√	√	√	√			
Design constraints	√					√	√	√

[1] Variable depends on the heat source temperature.
[2] Heat source temperature $T_{hs,in}$ is variable depends on the available heat source data.
[3] Heat sinks temperature T_{sink} = 301 K *(average annual water coolant temperature).*
[4] Pinch points for evaporator and condenser are both 5 K.
[5] Water cooled condenser.

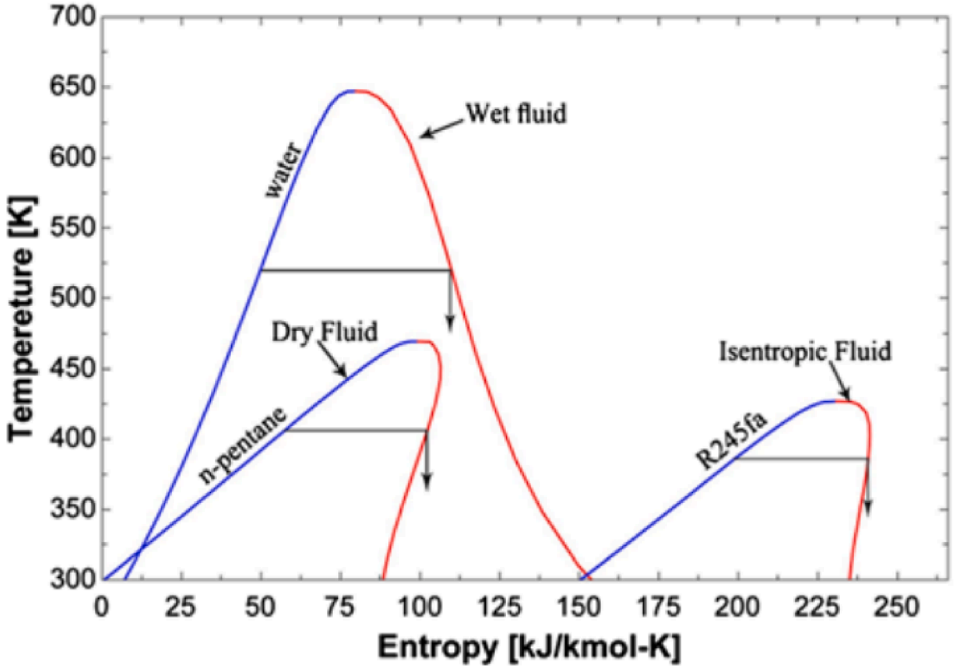

Fig. 2. Type of working fluids based on the slop of slope of the saturation vapor curve on a T-s diagram).

as a base for determining the design variables and constraints for the ORC unit of this study as shown in Table 2.

2.1. *T-s characteristic curves of the working fluids*

The working fluids can be categorized into three groups; dry, isentropic, or wet fluid depending on the slope of the saturated vapor curve on a T-s diagram (ds/dT) as depicts in Fig. 2. The slope of the saturated vapor curve is an important thermos-physical property of the working fluid, and it has a key impact on thermal efficiency and equipment arrangement [14]. In case of a wet fluid (e.g., water), the curve has a negative slope, i.e. the fluid will be in a two-phase mixture upon isentropic expansion which in most industrial applications required a superheating process to enhance the quality of the mixture and maintain the maximum allowed wetness at the turbine outlet and avoid blading erosion damage [15]. A dry fluid (e.g., n-pentane) has a positive slope of the saturated vapor curve where superheating is not necessary. The highest cycle efficiency of those working fluids can be achieved by keeping the saturated steam conditions at the turbine inlet [16,17]. From thermodynamic point of view, superheating the dry fluid leads to increase the temperature at the exit port of the turbine and consequently higher condenser load but unfortunately without having a significant impact on turbine power output [18]. The degree to which organic fluids are dry is generally related to their molecular weight or molecular complexity. For organic fluids, the larger the molecular weight, the greater is the slope of the T-s curve. The isentropic fluid has an infinitely large slope where entropy change is equal to zero. In other words, the vapor saturation line on a T-s diagram is vertical for these fluids [13]. For most of isentropic organic fluids, the isentropic expansion process will develop a superheated vapor at low and moderate temperatures at the exit port of the turbine. In other words, no attention needs to be paid to vapor quality at the end of the expansion process rather than a two-phase mixture as with water [19]. For ORC applications, dry or isentropic working fluids type are more appropriate where they will be in superheated vapor phase after isentropic expansion, thereby eliminating the concerns of impingement of liquid droplets on the turbine blades and making the superheated apparatus unnecessary [9].

2.2. *Environmental and safety characteristics of the working fluids*

During the design process of an ORC, the environmental and safety characteristics of working fluids should also be considered because they will have a significant influence on Unit operators' health and its environment. A good organic working fluid should achieve the environment and safety conditions in terms of low toxicity, lower Ozone Depletion Potential (ODP), lower Global Warming Potential (GWP), and longer

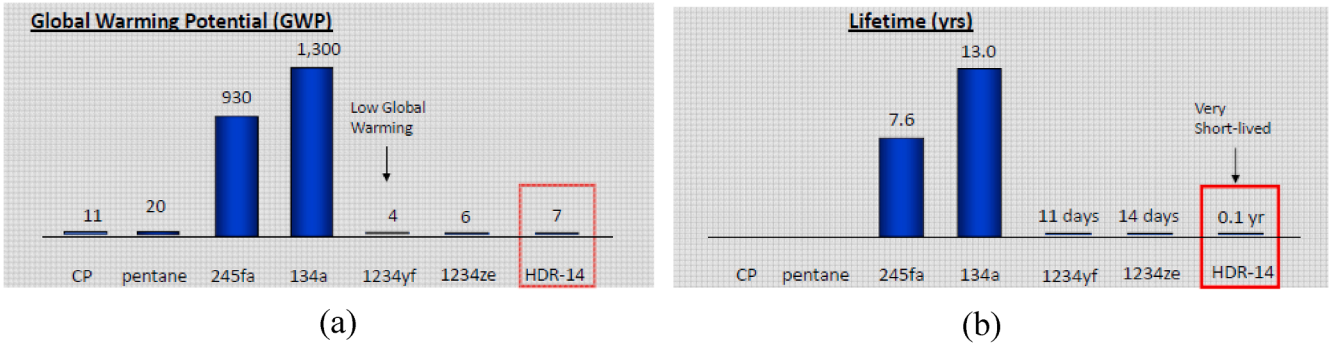

Fig. 3. a) global warming potential, b) lifetime (Zyhowski and Brown, 2015).

Table 3
Organic fluids selection criteria.

Criteria	Range			
	high	Moderate	Low	Remarks
Latent heat of vaporization	X			
Specific volume*			X	
Specific heat	X			
Critical temperature		X		
Critical pressure		X		
Slope (ds/dT) saturated vapor curve**				Zero or positive slope
Operating pressures (condensation & vaporization)				between 1 & 25 bar respectively
Viscosity***			X	
Thermal conductivity***	X			
Thermal and chemical stability	X			
Safety characteristics		X		
Environmental impact (ODP, GWP)			X	
Cost and availability			X	

* In the liquid-vapor phase.
*In these cases the fluids are termed as isentropic or dry fluids.
*** To provide good heat transfer.

Atmospheric Life Time (ATL) of operation. The ODP is the ratio of the impact on ozone of a chemical compared to the impact of a similar mass of R-11. Thus, the ODP of R-11 is defined to be 1.0. Normally, fluids have ODPs between 0.1 and 1 [20]. Working fluids which have higher ODP than zero cannot be considered for power generation due to restrictions on their use imposed by the Montreal protocols [21]. GWP represents how much a given mass of a chemical contributes to global warming over a given time period as compared to the same mass of carbon dioxide. Carbon dioxide's GWP is defined as 1.0. Thus, a fluid with GWP of 2 has the effect on global warming two times stronger compared to the CO_2. A GWP is calculated over a specific time interval, commonly 100 years [22]. ALT is the length of time that a gas will remain in the atmosphere based on its decay rate and its tendency and likeliness to react with other gases. To complement these indices, the maximum time-average concentration for a normal 8-h work day has also been presented as toxicological index [19,23]. Fig. 3 illustrates the environmental and safety characteristics of some working fluids. For instant, R134a has lifetime of 13 years in comparison to 7.6 years of R245fa while its GWP is approximately 40% greater than that of R245fa as shown in Fig. 3 [24].

2.3. Organic fluids selection criteria

Certain characteristics are important for the selection process of the organic fluids in ORC application. For instant, fluids having high latent heat and density could absorb more energy from the source in the evaporator, which in turn minmize the required fluid flow rate, and consequnetaly reduce the pump power consumption [25]. In terms of saturated vapor specific volume, it is prefered that the orgaic fluid to have a low specific volume which requires smaller condensing equipment. Therefore, fluids with high specific volume are not suitable for application due to the large size of the required condensing equipment. Table 3 sheds light on the most important characteristics of the organic fluid and their range.

In commercial applications the following organic fluids are found: Ammonia (R-717) used in geothermal power plants; R-245fa (HFC) for low temperatures; N-pentane used at the commercial solar-powered ORC plant in Nevada, USA; Solkatherm (SES36) which is an azeotropic mixture; Toluene for recovery at higher temperatures; Hydrocarbons (HCs), Hydrofluorocarbons (HFCs), Hydrofluoroethers (HFEs) and OMTS (octamethyltrisiloxane) [26]. Baral and Kim [27] analyzed thermodynamically fifteen organic fluids in an Organic Rankine Cycle, they found that RC318 and R123 have a very good performance, but more attention should be paid related to their environmental precautions as a result of the high ozone depletion power and high global warming power. In addition, the slop of the saturated vapor curve

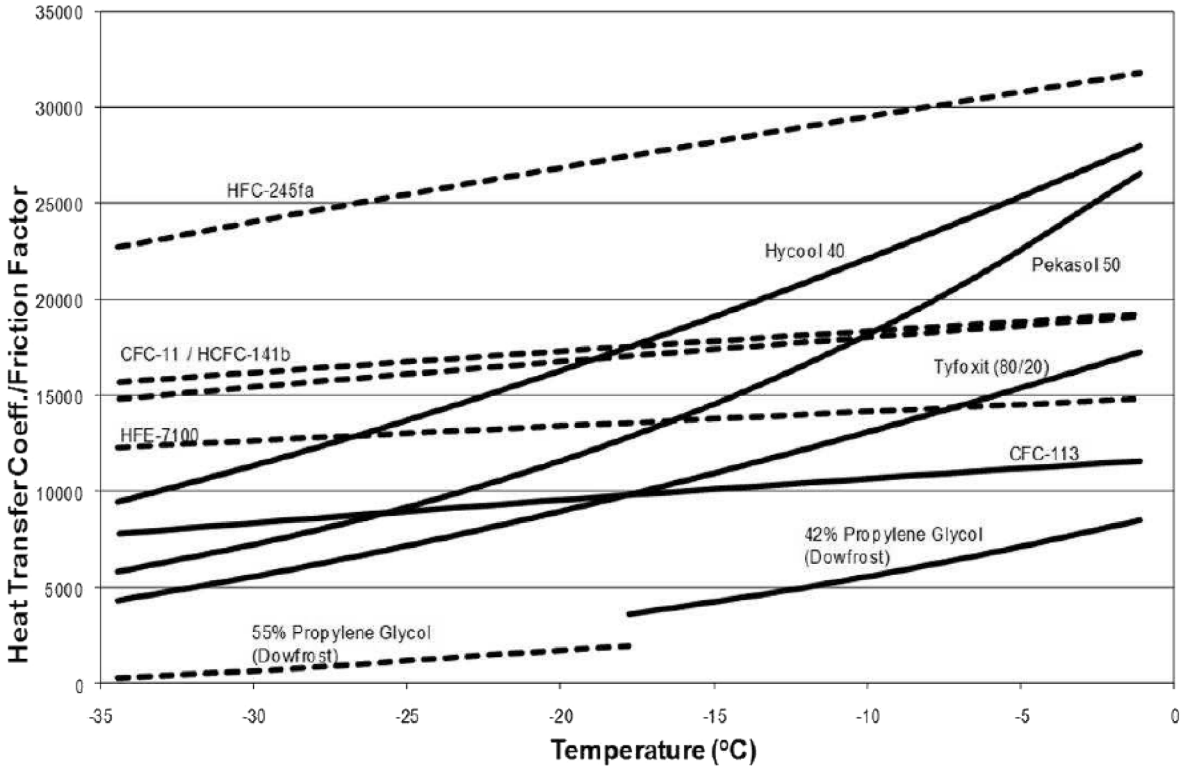

Fig. 4. Performance of heat transfer fluids, Source Honeywell [28].

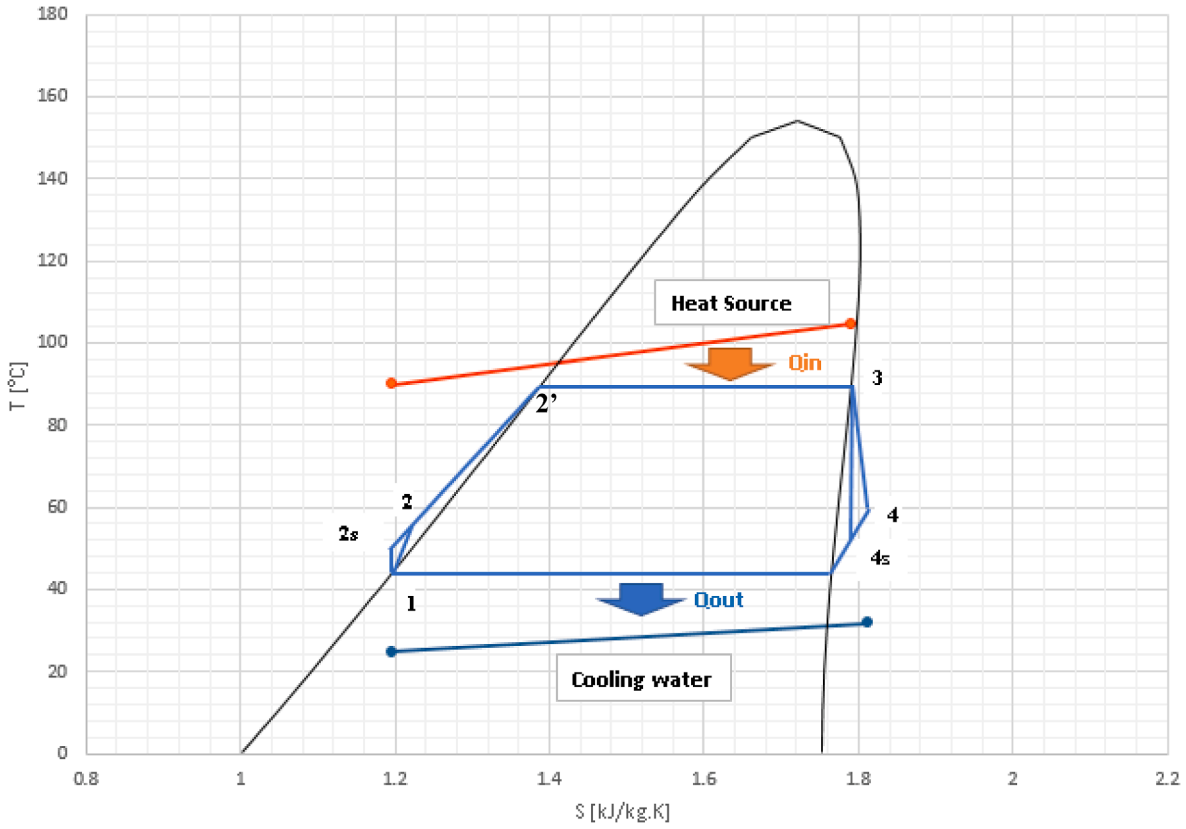

Fig. 5. Working principle layout of an ORC unit.

turned to positive when the temperature becomes less than 150 °C while it has negative slop at higher temperature range. The choice of an organic fluid that is suitable for ORC should achieve the following desirable characteristics; i) better operating conditions in terms of low specific volume, adequate critical low temperature and pressure, low viscosity, high thermal conductivity and working with moderate pressures; ii) environment and safety conditions in terms of low toxicity, lower Ozone Depletion Potential (ODP), lower Global Warming Potential (GWP), and longer life time of operation, adequate thermal stability and compatible with turbine material and lubricating oil. Accordingly, and based on the temperature range of the available waste heat sources of the current study the refrigerant (R-245fa) is selected to be the working fluid. The use of R245fa would provide profitable performance in terms of high heat exchanger efficiency and low pump power requirements which can be expressed by the ratio of heat transfer coefficient to friction factor. According to Honeywell data R245fa has a higher heat transfer coefficient to friction factor ratio than many other commercially available organic fluids as shown in Fig. 4. In addition, it should be noted that R245fa, operate at super-atmospheric pressure at condenser temperature of 40 °C, which is beneficial for small-scale applications to eliminate infiltration of non-condensable gases.

3. ORC unit modeling methodology

3.1. Model approach

Fig. 5 depicts the layout working principle of the ORC unit. The condensate low pressure refrigerant is pumped from the condenser outlet to the high pressure at the evaporator inlet where the heat recovering process is started. For the ideal cycle, the compression process is modeled as an isentropic process (reversible and adiabatic process). In the evaporator, the refrigerant absorbs the thermal energy from industrial waste heat sources at approximately constant pressure. In this process, the refrigerant undergoes a phase change from compressed liquid to saturated or superheated vapor. The high pressure saturated or superheated vapor undergoes an expansion process through the expander at isentropic conditions to produce the shaft work. During the expansion process, the pressure decreases to the condenser pressure where the refrigerant enters the condenser as a saturated or superheated vapor depending on working conditions and the type of refrigerant at use. In the condenser, the refrigerant condensates and changes phase to saturated or undercooled liquid with the help of a heat sink. The cycle is then repeated. The actual cycle differs from the ideal one on several accounts. In an actual cycle, the compression and expansion processes, in fact, are not isentropic and there is always irreversibility present due to entropy generation whether internally as the internal transfer of energy over a finite temperature difference in the components or externally due to the mechanical losses during work transfer and heat transfer over the finite temperature difference [29]. Some pressure drop due to friction in the system associated pipes during heat addition and heat rejection processes are also inevitable.

3.2. Assumptions and limitations

To perform the analysis for the ORC, some idealizations and simplifications are employed as the following:

a) *Constant pressure heat addition and heat rejection process*

The refrigerant does not experience any pressure drop due to friction or minor losses when passing through the piping system, evaporator and condenser.

b) *Quasi-equilibrium manner*

All expansion and compression processes take place in a quasi-

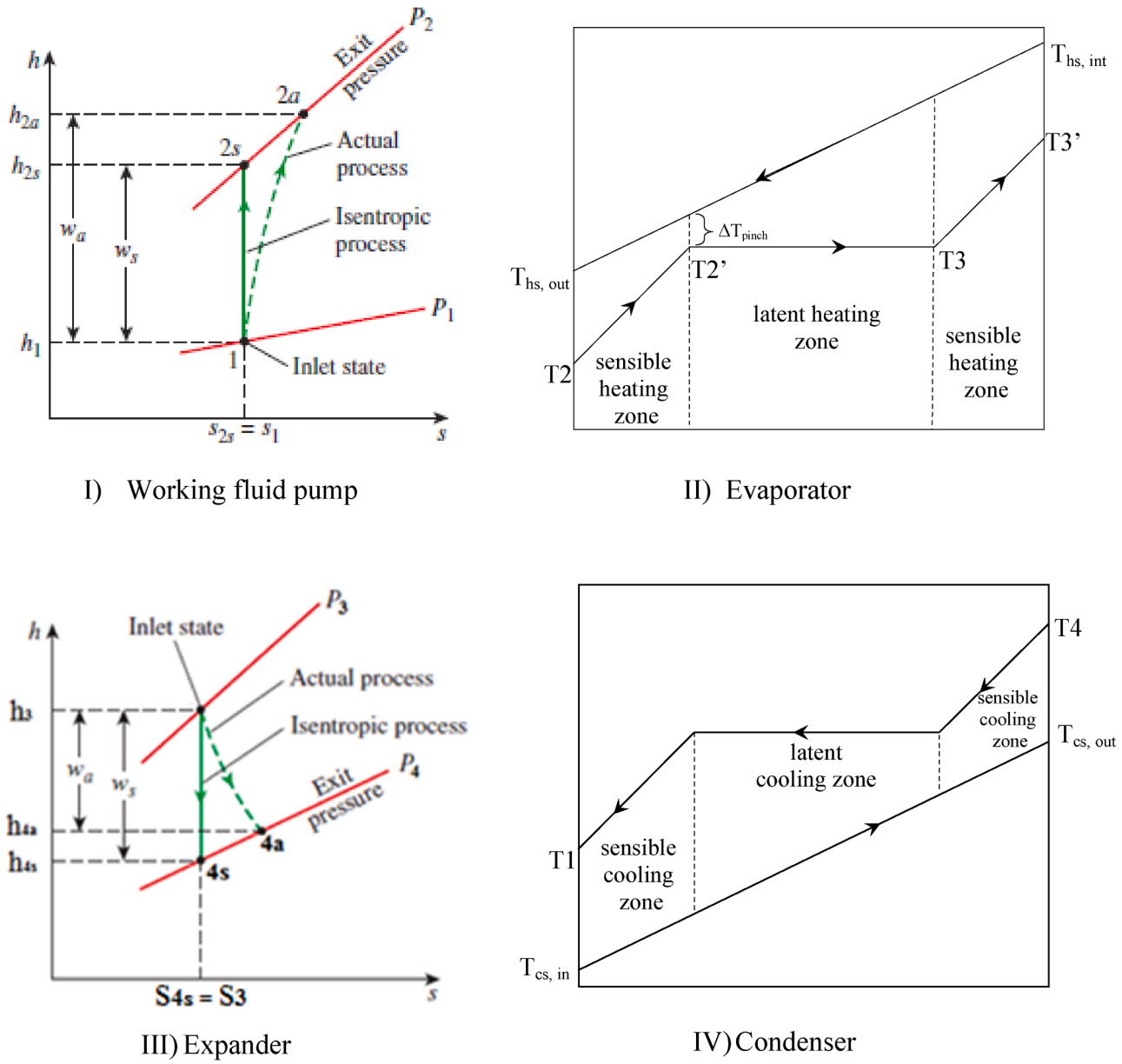

Fig. 6. The h-s diagram for the actual and isentropic processes of ORC components.

equilibrium manner. The work-producing devices deliver the most work when they operate in quasi-equilibrium processes. Therefore, quasi-equilibrium processes serve as standards to which actual processes can be compared [29].

c) *Adiabatic compression and expansion processes in the piping system*

The pipes connecting the components are well insulated. Therefore, the heat transfer is negligible through them.

d) *Changes in kinetic and potential energies of the refrigerant are neglected*

This is a reasonable assumption made in devices that involve shaft work such as turbines and pumps; the kinetic energy and potential energy terms are usually very small relative to the other terms in energy equation. In other words, a very high speed (≈ 500 m/s) is required to make a 1 kJ/kg of kinetic energy change and a potential energy change of 1 kJ/kg corresponds to an elevation difference of 102 m. In addition, fluid velocities in evaporator and condenser are typically low making kinetic energy changes negligible [29].

e) *Steady state processes*

The operation state in the design model is considered to be at steady state.

f) *No work interactions*

The heat exchangers involve no work interactions.

g) *Counter flow heat exchangers*

The evaporator and condenser are assumed to be counter flow heat exchangers due their significant advantages over parallel flow heat exchanger. In other words, the counter flow heat exchanger has more uniform temperature difference between the hot and the cold streams which could develop uniform heat transfer rate and minimize the thermal stress throughout the exchanger. Furthermore, there is a

possibility for the outlet temperature of the cold stream to approach the highest temperature of the hot stream.

3.3. System equations and thermodynamic analysis

The design model is primarily based on setting up mass and energy balances on system components, which are: the pump, the evaporator, the expander and the condenser. The thermodynamic cycle is closed and continuous. Therefore, each component analysis has to be in consistent with the others. In addition, the cycle involves two external open cycles, one is used as a heat source and the other is used for cooling purposes. The model is constructed using the fundamentals concepts of thermodynamics, heat transfer and fluid mechanics (Eqs. (1)–(4)) for each individual component as depicts in parts I to IV using the h-s diagram of ORC components is shown in Fig. 6. Pinch points for evaporator and condenser are considered to 5 K. The pinch point limitation leads to a lower evaporating pressure and thus to a lower cycle efficiency, but with an increase in the amount of heat recovered as well as the output power. This limitation highlights the necessity of a pinch point analysis for a given application. In general, in heat recovery applications, the objective will be to maximize the output power rather than the efficiency.

$$\sum_{in}\dot{m} = \sum_{out}\dot{m}\left(\frac{dm_{CV}}{dt} = 0 for steady state flow\right) \tag{1}$$

$$\dot{m}_{ref,i} = \dot{m}_{ref,i+1} = \dot{m}_{ref} \tag{2}$$

$$\dot{E}_{in} = \dot{E}_{out}\left(\frac{dE_{system}}{dt} = 0 for steady state process\right) \tag{3}$$

$$\dot{W}_{net,in} - \dot{Q}_{net,out} = \Delta H + \Delta KE + \Delta PE\left(\Delta KE \approx 0; \Delta PE \approx 0; isentropic\right) \tag{4}$$

I) Working fluid pump (1–2 compression process)

$$\dot{W}_p = \dot{m}_{ref}(h_2 - h_1) \tag{5}$$

The isentropic efficiency is used to find the actual enthalpy h_{2a} using h_{2s} as the following:

$$(\eta_s)_{pump} = \frac{w_s}{w_a} = \frac{h_{2s} - h_1}{h_{2a} - h_1} \tag{6}$$

II) Evaporator (2–3 constant pressure heat addition process)

$$\dot{Q}_{net,in} - \dot{W}_{net,out} = \Delta H\left(\dot{W}_{net,out} \approx 0\right) \tag{7}$$

$$\dot{Q}_{ref} = \dot{m}_{ref}(h_3 - h_2) \tag{8}$$

$$\dot{Q}_{HS} = \dot{m}_{HS} c_{p,HS} \Delta T_{HS} \tag{9}$$

$$\varepsilon = \frac{Actual heat transfer}{m maximun supplied heat} = \frac{\dot{Q}_{ref}}{\dot{Q}_{HS}} \tag{10}$$

$$\dot{Q}_{ref} = 0.98\dot{Q}_{HS}\left(heat exchanger effectivness is assumed to be 0.98\right) \tag{11}$$

III) Expander (3–4 expansion process)

$$\dot{W}_{exp} = \dot{m}_{ref}(h_3 - h_4) \tag{12}$$

The isentropic efficiency is used to find the actual enthalpy h_{4a} using h_{4s} as the following:

$$(\eta_s)_{exp} = \frac{w_a}{w_s} = \frac{h_3 - h_{4a}}{h_3 - h_{4s}} \tag{13}$$

$$\dot{W}_{exp} = (\eta_s)_{exp}\dot{m}_{ref}(h_3 - h_{4a}) \tag{14}$$

IV) Condenser (4–1 constant pressure heat rejection process)

$$\dot{W}_{net,in} - \dot{Q}_{net,out} = \Delta H\left(\dot{W}_{net,in} \approx 0\right) \tag{15}$$

$$\dot{Q}_{ref,cond} = \dot{m}_{ref}(h_4 - h_1) \tag{16}$$

$$\dot{Q}_C = \dot{m}_C c_{p,C} \Delta T_C \tag{17}$$

The reversible thermal efficiency of the cycle is clouted as per Eq. (18)

$$\eta_{th,rev} = 1 - \frac{T_L}{T_H} \tag{18}$$

3.4. Solution algorithm

The following steps have been followed to establish the solution algorithm of the ORC unit using MATLAB software and CoolProp library. The library was able to access *R-245fa* thermodynamic properties required for the calculations. In the calculation, the pinch points for evaporator and condenser are considered to 5 K. The pinch point limitation leads to a lower evaporating pressure and thus to a lower cycle efficiency, but with an increase in the amount of heat recovered as well as the output power. This limitation highlights the necessity of a pinch point analysis for a given application. In general, in heat recovery applications, the objective will be to maximize the output power rather than the efficiency.

1. State pump inlet temperature T_1 is obtained by considering the design limit of pinch temperature at the condenser outlet (sat. vapor line) and the estimated outlet temperature of the coolant water stream. For instant @ water coolant temperature of 30 °C in May, and by estimating the temperature difference across the condenser of the coolant water to be about 8 °C, T_1 in such circumstances equals to 38 °C. The condition of the design pinch temperature at the condenser outlet should be checked.
2. Using T_1 and quality ($x = 0$) at the saturated liquid line of the refrigerant, the low pressure of the cycle is determined using the saturated liquid curve of the refrigerant. For ($T_1 = 38$ °C, $x = 0$) the condenser pressure is found to be 0.236 MPa, $h_1 = 250.38$ kJ/kg, $s_1 = 1.1727$ kJ/kg. K.
3. The refrigerant thermodynamics properties (*enthalpy an entropy*) at state are calculated using saturated data of the refrigerant at calculated pressure (*low pressure*) in step 2.
4. State could either be a saturated vapor phase or superheated vapor phase. For simplicity the thermal analysis, state considered to be saturated vapor. The temperature is calculated by subtracting the estimated temperature difference value (10 °C) across the heat source stream from the maximum temperature of the available waste heat source. For instant at ACAW Power Barka I, the temperature T_3 is found to be 95 °C. Using the temperature of the waste heat source and the design pinch temperature at the evaporator outlet, the temperature of the refrigerant at state should be checked.
5. Using T_3 and quality ($x = 1$) at the saturated vapor line of the refrigerant, the high pressure of the cycle is determined using the saturated liquid curve of the refrigerant. For ($T_3 = 95$ °C, x = 1) the evaporator pressure is found to be 1.1274 MPa, $h_3 = 473.68$ kJ/kg, $s_3 = 1.7956$ kJ/kg. K.
6. Considering the isentropic efficiency and using the properties found in step 2 and high pressure in step 5, the thermodynamics properties of the refrigerant at state are calculated, i.e. at ($s_2 = s_1$. $P_2 = P_3$) and then Eq. (6) is used to calculate h_{2a}.
7. Considering the isentropic efficiency of the expander and using the properties found in step 5 and the low pressure in step 2, the thermodynamics properties of the refrigerant at state are calculated, i.e.

Table 4
ORC properties characteristics.

Properties		Property's type in the mathematical model			
		Input	Estimated	Calculated	Output
Variable parameters	Heat source Mass flow rate, [kg/s]	√			
	Heat source temperature, [°C]	√			
	Cooling source temperature, [°C]	√			
	Specific heat capacity, [kJ/kg.°C]	√			
	Dimensionless mass flow rate ratio		√		
Constant parameters	Pinch temperature, [°C]		√		
	Expander isentropic efficiency [%]		√		
	Pump isentropic efficiency [%]		√		
	Effectiveness [%]		√		
Calculated parameters	Temperature difference [°C]		√		
	Refrigerant mass flow rate, [kg/s]			√	
Pump inlet	T_1, [°C]			√	
	P_{low}, [kPa]			√	
	h_1, [kJ/kg]			√	
	s_1, [kJ/kg.°C]			√	
Pump outlet	T_2', [°C]			√	
	P_{high}, [kPa]			√	
	T_2, [°C]			√	
	h_{2s}, [kJ/kg]			√	
	h_{2a}, [kJ/kg]			√	
	s_2, [kJ/kg.°C]			√	
ExpanderInlet	T_3, [°C]			√	
	h_3, [kJ/kg]			√	
	s_3, [kJ/kg.°C]			√	
Expander Outlet	h_{4s}, [kJ/kg]			√	
	h_{4a}, [kJ/kg]			√	
	T_4, [°C]			√	
	s_4,[kJ/kg.°C]			√	
The entire unit	Amount of heat input, [kW]				√
	Amount of rejected heat, [kW]				√
	Compression work, [kW]				√
	Expansion work, [kW]				√
Parasitic load	Cooling source mass flow rate, [kg/s]			√	
	Cooling source pressure, [kPa]		√		
	Cooling source pump work, [kW]			√	
Performance parameters	Net work output, [kW]				√
	Actual Thermal efficiency; [%]				√
	Reversible thermal efficiency, [%]				√

at ($s_4 = s_3$; $P_4 = P_1$), the enthalpy h_{4a} is then calculated using Eq. (13).

8. Using the thermodynamic properties that are obtained at each state of the ORC and using the fundamental thermodynamics equations of each component, the output parameters e.g. net work output, and thermal efficiency are calculated. Table 4 summarizes the ORC properties characteristics.

4. Results and discussion

4.1. Influence of the refrigerant mass flow rate

A dimensionless mass flow rate parameter (M) is used to study the influence of the refrigerant mass flow rate on the ORC performance with respect to mass flow rate of the hot fluid at the waste thermal energy source. It represents the ratio of the refrigerant mass flow rate to the waste heat source mass flow rate ($M = (\dot{m}_{ref}/\dot{m}_{hs})$). For better evaluation, four cases have been selected with variable heat source temperatures and mass flow rates while the cooling water temperature was kept constant at the average annual value of 28 °C.

Case a: high heat source temperature and high mass flow rate

$T_{hs} = 105^oC \& \dot{m}_{hs} = 4.69\frac{kg}{s}; T_{cs} = 28^oC$

Case b: high heat source temperature and low mass flow rate

$T_{hs} = 105^oC \& \dot{m}_{hs} = 0.975\frac{kg}{s}; T_{cs} = 28^oC$

Case c: low heat source temperature and high mass flow rate

$T_{hs} = 80^oC \& \dot{m}_{hs} = 4.69\frac{kg}{s}; T_{cs} = 28^oC$

Case d: low heat source temperature and low mass flow rate

$T_{hs} = 80^oC \& \dot{m}_{hs} = 0.975\frac{kg}{s}; T_{cs} = 28^oC$

The presented results in Fig. 7 showed that the dimensionless mass flow rate has a significant influence on the ORC thermal performance in terms of thermal efficiency and net power output.

For cases *(a)* and *(b)* of high temperature waste heat sources, it has been observed that increasing the dimensionless mass flow rate causes the net power output to increase while the thermal efficiency decreases. The plausible reason for such a trend is that, as the low pressure at the condenser inlet was fixed in all cases, the net power produced will be solely depend on the thermodynamic state at the inlet of the expander, i.e. the higher temperature of the waste heat source allows the ORC cycle to operate at high pressure at the evaporator and achieve a higher value for superheating. Thermodynamically, this increases the area under the *T-s* and *P-v* diagrams, consequently higher power output would be expected. Although, high refrigerant temperatures can be reached at the expander inlet, the actual heat transfer from heat source to refrigerant in the evaporator may become more effective depending on the corresponding $\dot{m}_{ref}$ used. This would diminish the thermal efficiency as per ($\eta_{th} = (\dot{W}_{net}/\dot{Q}_{in})$). For cases *(c)* and *(d)* in Fig. 7, the thermal efficiency follows the same trend as in cases *(a)* and *(b)*. However, the net power output peaks when M reaches an approximately 0.4 and decreases sharply with increasing M values. Such a trend in work net output can be attributed to the critically low pressure ratio between the evaporator pressure (P_{high}) and condenser pressure (P_{low}) after M passes 0.4. This is clearly illustrated in Fig. 8b which corresponds to cases (*c*) and (*d*). The low pressure ratio affects the net power output by decreasing the area under the *T-s* and *P-v* diagrams. In other words, the decreasing in pressure ratio develop a significant decreasing in the power produced by the expander ($W_{exp} = h_3 - h_4$) as shown in Fig. 9b, consequently a low net power output would be achieved. However, for waste heat sources of high temperatures as in cases (*a*) and (*b*), the pressure ratio as well as the enthalpy difference across the expander remain at high values for all values of M as shown in Fig. 8a and Fig. 9a. It can be concluded that, the refrigerant mass flow rate ($\dot{m}_{ref}$) plays a decisive role in determining the pressure level at the evaporator hence it is a critical factor for the power production capability of the ORC unit. For this study, the optimum mass flow rate ratio was selected to be 0.35 which is represented a

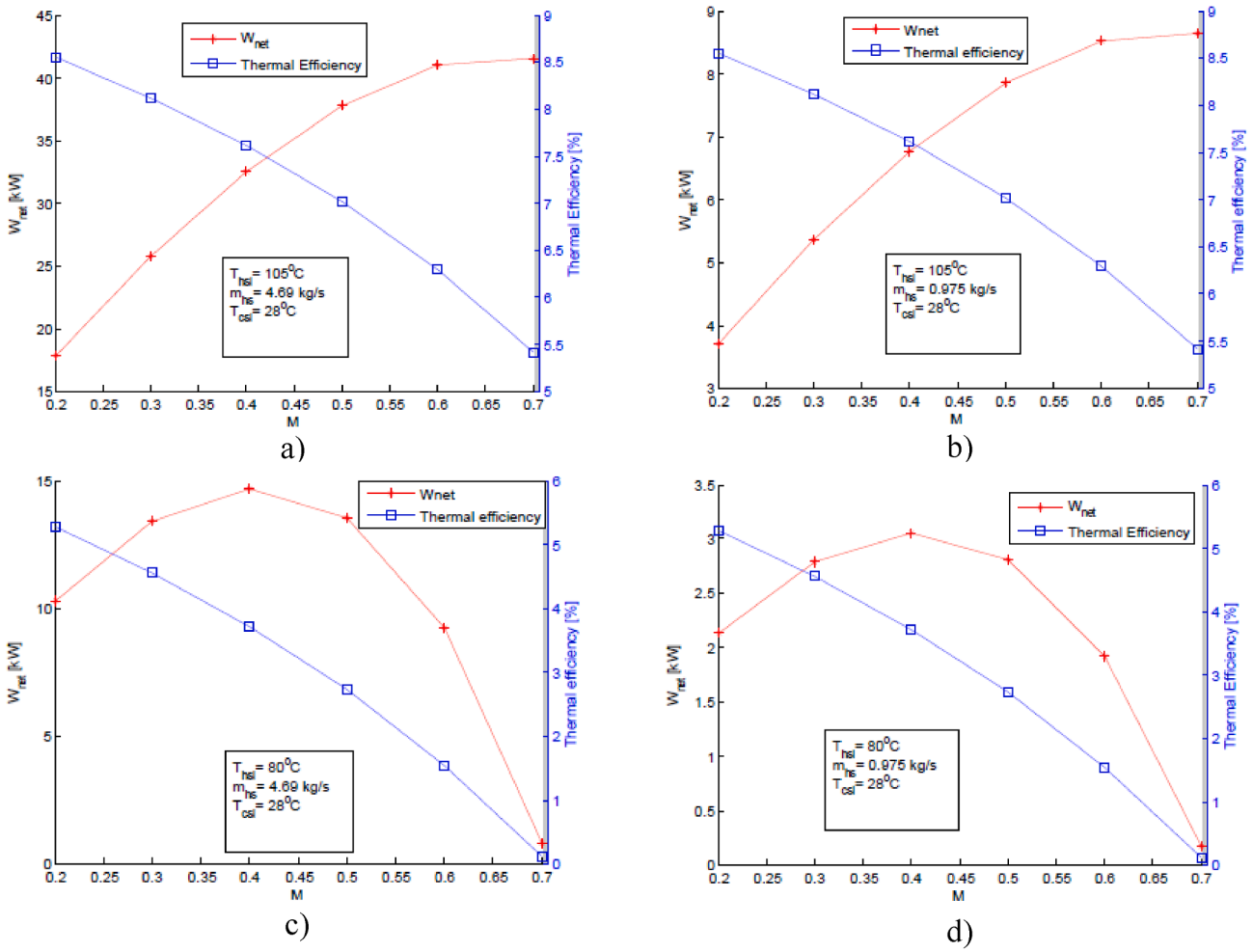

Fig. 7. Dimensionless mass flow rate versus ORC performance for *a)* waste heat source of high temperature and flow rate, *b)* waste heat source of high temperature and low flow rate, *c)* waste heat source of low temperature and high flow rate, *d)* waste heat source of low temperature and flow rate.

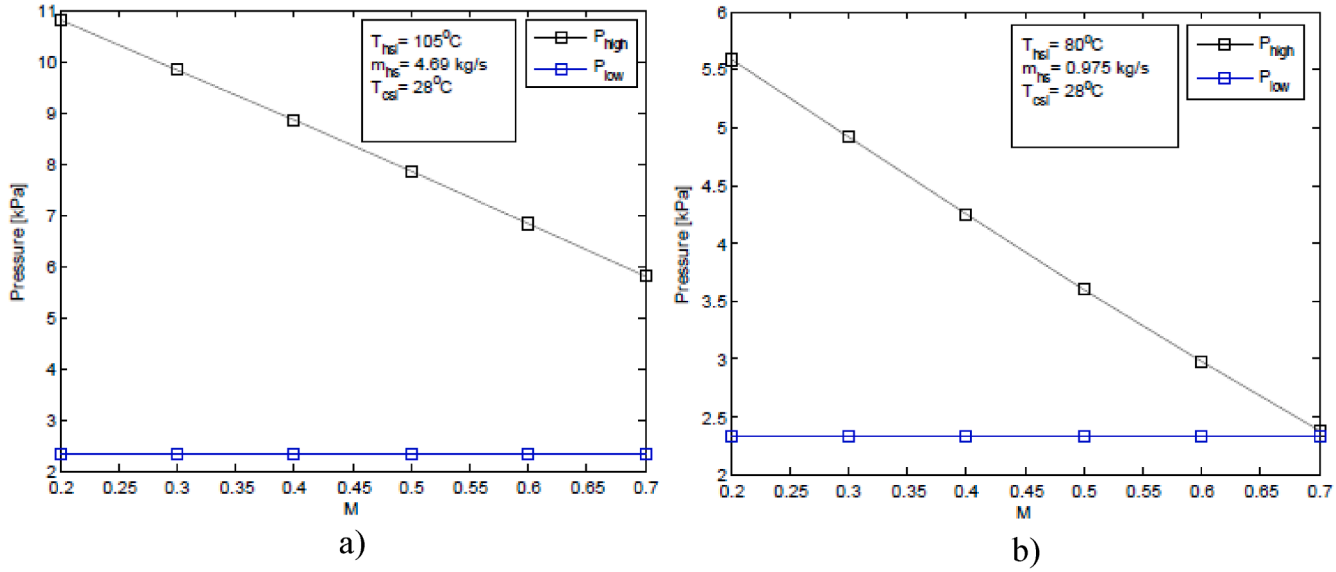

Fig. 8. Dimensionless mass flow rate versus pressure for, *a)* high pressure ratio *b)* low pressure ratio.

compromised solution for all four cases that show optimum values between 0.25 and 0.45.

Based on the data from Al Rusail Power Plant, the optimum mass flow rate ratio is at approximately M at 0.15 as shown in Fig. 10, therefore, this considered to be the design value for this special case.

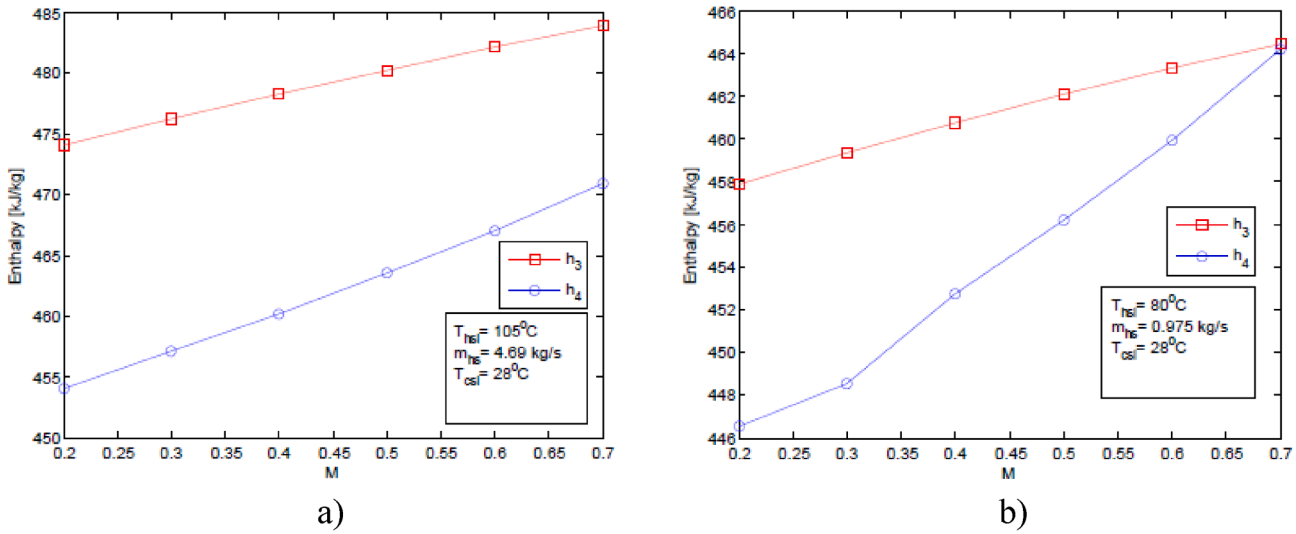

Fig. 9. Dimensionless mass flow rate versus enthalpy *(h_3 & h_4)* for, *a)* waste heat source of high temperature, b) waste heat source of low temperature.

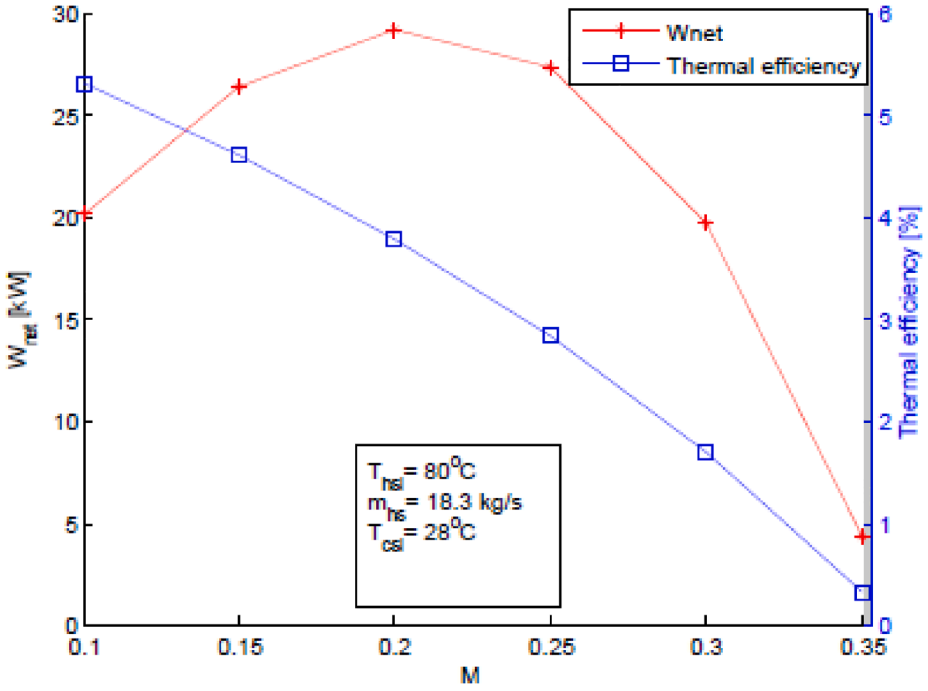

Fig. 10. Dimensionless mass flow rate versus ORC performance for *Al Rusail Power Plant.*

Table 5
Annual water coolant temperature in Oman, °C (seatemperature.org).

Jan	Feb	Mar	Apr	May	Jun	Jul	Aug	Sep	Oct	Nov	Dec
24.2	23.3	24.7	26.8	30.0	31.6	31.5	30.9	30.3	29.6	27.9	25.7

Lowest recorded temperature: February at 22.3 °C.
Highest recorded temperature: July at 33.5 °C.
Average annual temperature: 28 °C.

4.2. Influence of water coolant temperature

The influence of the water coolant temperature represented in Table 5 (seatemperature.org) on the ORC performance has been thermally evaluated using the available waste heat temperature of each industry and the optimum mass flow rate ratio obtained in the previous section. The evaluation presented in terms of heat gain, heat rejected, variation in overall thermal efficiency and net power output for the selected industries (*ACWA Power Barka I, Areej Vegetable Oil & Derivatives, Al Ghubra Power & Desalination, and Al Rusail Power Plant*) as shown in Tables 6–9. A closer look at the data, it can be observed that, higher thermal performance could be achieved at the first and the last

Table 6
Influence of cooling water temperature on ORC performance at *ACWA Power Barka.*

ACAW Power Barka I						
T_{hsi} (°C)		105		m_{hs} (kg/s)		4.69
M		0.35		m_{ref} (kg/s)		1.6415
Month	$T_{cs,i}$ (°C)	Q_{in}, kW	Q_{out}, kW	W_{net}	η_{th}, %	η_{rev} %
Jan	24.2	391.23	361.63	29.60	7.57	21.37
Feb	23.3	418.85	388.58	30.27	7.23	21.61
Mar	24.7	419.64	390.42	29.22	6.96	21.23
Apr	26.8	403.96	376.28	27.68	6.85	20.68
May	30	374.81	349.47	25.34	6.76	19.83
Jun	31.6	362.24	338.07	24.17	6.67	19.41
Jul	31.5	364.82	340.55	24.27	6.65	19.44
Aug	30.9	357.83	333.14	24.68	6.90	19.60
Sep	30.3	339.85	314.71	25.14	7.40	19.75
Oct	29.6	331.87	306.26	25.61	7.72	19.94
Nov	27.9	338.79	311.91	26.88	7.93	20.39
Dec	25.7	365.51	337.02	28.49	7.79	20.97

Table 7
Influence of cooling water temperature on ORC performance at *Areej Vegetable Oils & Derivatives.*

Areej Vegetable Oils & Derivatives						
T_{hsi} (°C)		80		m_{hs} (kg/s)		0.975
M		0.35		m_{ref} (kg/s)		0.34
Month	$T_{cs,i}$ (°C)	Q_{in}, kW	Q_{out}, kW	W_{net}	η_{th}, %	η_{rev} %
Jan	24.20	78.27	75.23	3.04	3.88	15.80
Feb	23.30	91.88	88.70	3.18	3.46	16.06
Mar	24.70	94.48	91.51	2.97	3.14	15.66
Apr	26.80	87.93	85.29	2.64	3.01	15.06
May	30.00	75.08	72.91	2.17	2.89	14.16
Jun	31.60	69.19	67.25	1.93	2.79	13.71
Jul	31.50	70.25	68.31	1.94	2.77	13.73
Aug	30.90	66.37	64.33	2.04	3.07	13.90
Sep	30.30	57.84	55.71	2.12	3.67	14.07
Oct	29.60	54.83	52.61	2.22	4.06	14.27
Nov	27.90	57.42	54.94	2.48	4.32	14.75
Dec	25.70	67.64	64.83	2.81	4.16	15.38

Table 8
Influence of cooling water temperature on ORC performance at *Al Ghubra Power & Desalination.*

Al Ghubra Power & Desalination						
T_{hsi} (°C)		115		m_{hs} (kg/s)		4.394
M		0.35		m_{ref} (kg/s)		1.54
Month	$T_{cs,i}$ (°C)	Q_{in}, kW	Q_{out}, kW	W_{net}	η_{th}, %	η_{rev} %
Jan	24.20	364.23	331.73	32.49	8.92	23.39
Feb	23.30	366.28	333.13	33.14	9.05	23.62
Mar	24.70	363.26	331.10	32.15	8.85	23.26
Apr	26.80	359.26	328.55	30.71	8.55	22.72
May	30.00	352.41	323.90	28.51	8.09	21.90
Jun	31.60	349.03	321.60	27.43	7.86	21.49
Jul	31.50	348.84	321.37	27.47	7.88	21.51
Aug	30.90	350.39	322.49	27.90	7.96	21.67
Sep	30.30	351.69	323.39	28.30	8.05	21.82
Oct	29.60	352.82	324.06	28.76	8.15	22.00
Nov	27.90	356.93	326.97	29.95	8.39	22.44
Dec	25.70	361.21	329.73	31.47	8.71	23.01

quarters of the year. This can be attributed to the lower temperature of coolant water during winter seasons especially in January, February, March, November and December. Unfortunately, the ORC performance faced a significant deterioration during summer as a result of increasing in water coolant temperature especially in June, July and August. The increase in water coolant temperature will directly affect the operating process of the ORC by limiting the lower pressure at the condenser and consequently the work net (area under the P-v diagram) will decrease,

Table 9
Influence of cooling water temperature on ORC performance at *Al Rusail Power Plant.*

Al Rusail Power Plant						
T_{hsi} (°C)		80		m_{hs} (kg/s)		18.3
M		0.15		m_{ref} (kg/s)		2.745
Month	$T_{cs,i}$ (°C)	Q_{in}, kW	Q_{out}, kW	W_{net}	η_{th}, %	η_{rev} %
Jan	24.2	587.36	564.43	22.94	3.91	15.80
Feb	23.3	592.27	568.20	24.07	4.06	16.06
Mar	24.7	586.21	563.89	22.32	3.81	15.66
Apr	26.8	579.57	559.74	19.83	3.42	15.06
May	30	565.69	549.72	15.97	2.82	14.16
Jun	31.6	558.99	544.89	14.09	2.52	13.71
Jul	31.5	559.54	545.33	14.21	2.54	13.73
Aug	30.9	560.16	545.29	14.86	2.65	13.90
Sep	30.3	563.47	547.88	15.59	2.77	14.07
Oct	29.6	566.46	550.02	16.44	2.90	14.27
Nov	27.9	572.36	553.95	18.41	3.22	14.75
Dec	25.7	579.62	558.60	21.01	3.63	15.38

which in turn, creates a significant influence on the overall thermal efficiency ($\eta_{th} = (\dot{W}_{net}/\dot{Q}_{in})$). At high ambient temperatures, the system performance deteriorated and the net power output deviated from the nominal value by more than 30%. General conclusion is that, the water coolant temperature plays a decisive role on the performance of the ORC unit as presented in the significant fluctuations in both net power output and thermal efficiency.

4.3. ORC performance at the selected industries

The collected industrial data were used as input to the ORC model to evaluate their performance in terms of net power output and thermal efficiency using the average annual water coolant temperature (28 °C) as shown in Fig. 11.

It was found that the designed ORC unit is inapplicable for *Sharq Sohar Steel Rolling Mills* since the provided waste heat's temperature (60 °C) was too low to provide a sufficient output power. In addition, the required parasitic load for the coolant water and ORC working fluid pumps were greater than the work output of the expander. This means that the ORC unit at this location would consume more power than it can possibly provide. However, higher temperature values of the waste heat source provide greater net power output and thermal efficiency due to the possibility of the ORC unit to work at high evaporator pressure, which in turn, increases the area under the *P-v* diagram as consequently high power output could be developed. This is clearly shown in Fig. 12, from which the increasing in performance values with increasing the temperature of the waste heat source can be clearly observed, e.g. *Areej Vegetable Oils & Derivatives* (80 °C), *Al Rusail Power Plant* (80 °C), *ACWA Power Barka I* (105 °C) and *Al Ghubra Power & Desalination* (115 °C), respectively. Quantitative analysis showed that, *Al Ghubra Power and Desalination* provides the highest net power output and thermal efficiency of 29.9 kW and 8.37%, respectively, while 26.8 kW and 7.21% were the performance output at *ACWA Power Barka I.* 12.1 kW and 3.18% were the performance output at *Al Rusail Power Plant.* The ORC unit at *Areej Vegetable Oil & Derivatives* experienced a low thermal performance of 2.46 kW and 3.44%, however, *Areej Vegetable Oil & Derivatives* has a higher thermal efficiency than *Al Rusail Power Plant.* This is due to *Al Rusail Power Plant* required higher water coolant flow rate which affects the coolant pumping work that is deducted from the overall net power output thus affecting the thermal efficiency. Fig. 12 shows the comparison of the actual thermal efficiencies and the Carnot reversible efficiencies. For even the highest heat source value provided by *Al Ghubra Power and Desalination* the thermal efficiency of the ORC does not exceed 10%, this is consistent with the results presented by [11]. The large difference between the reversible and actual thermal efficiencies show that improvements can be made to increase the overall actual thermal efficiency by minimizing thermal losses.

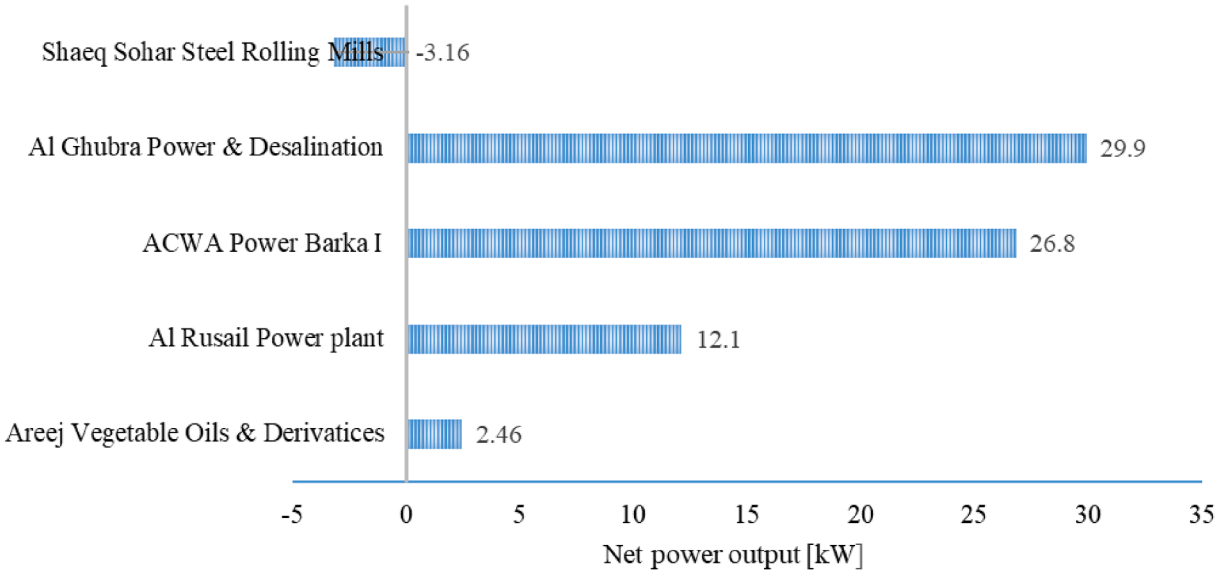

Fig. 11. ORC performance of the selected industries in terms of net power output.

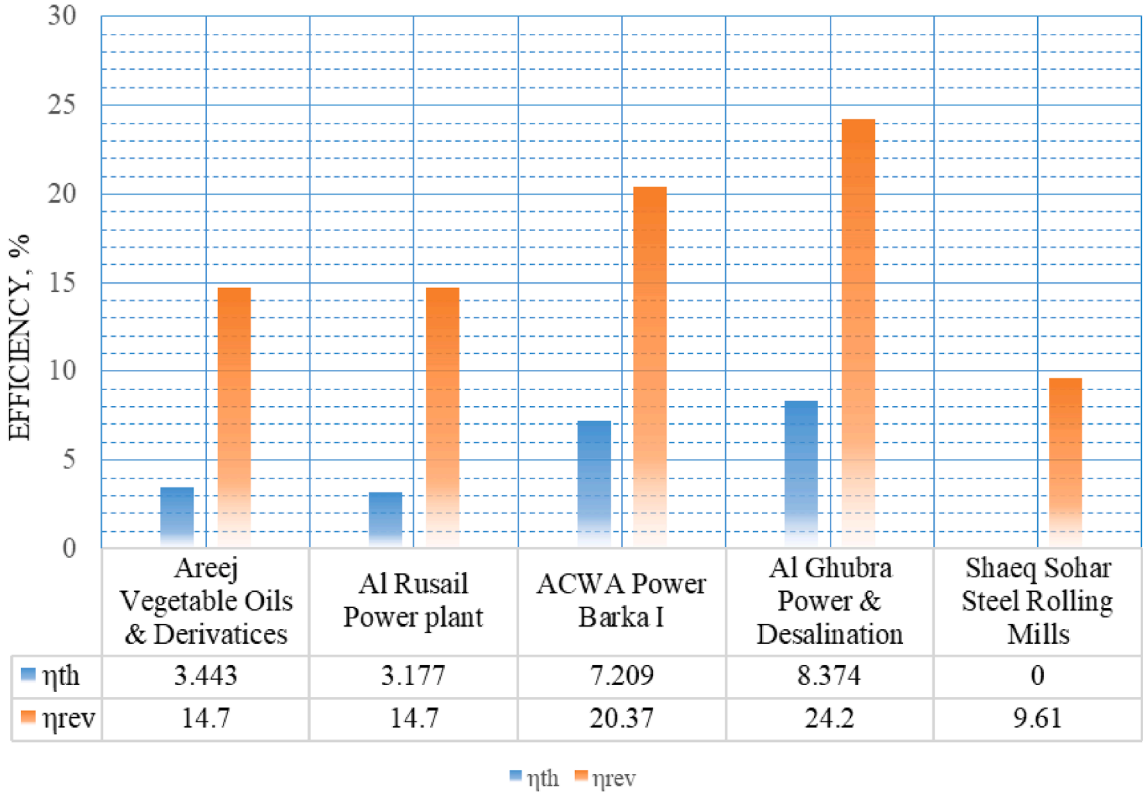

Fig. 12. ORC performance of the selected industries in terms of thermal efficiency and Carnot reversible efficiency.

5. The economic feasibility of implementing ORC

The attractiveness of utilization of ORC as a heat recovery technology depends on the Payback Period (PBP) offered to the end user and EBITDA "stands for Earnings Before Interest, Taxes, Depreciation, and Amortization" which is defined as a metric used to evaluate a company operating performance. There two business scenarios for implementing ORC in Oman. Scenario # 1, the industrial company itself invests in the installation of an ORC unit to supply its factory with electrical energy by converting the available waste heat. The investment is paid back from the expected savings on the energy bill. Scenario # 2, A second partner (investor) will install an ORC unit to produce an additional power by recovering the available waste heat at the first partner (industrial company) and sell it to the grid at the actual market price. In this case, the revenue of the second partner depends on the price at which the grid purchases the energy produced by the ORC plant, while the revenue of the first partner is related to the selling of the available waste thermal energy (kW_{th}). Based on thermal performance of ORC at the selected companies, ACWA Power Barka I, Areej Vegetable Oil & Derivatives, Al Ghubra Power & Desalination, and Al Rusail Power Plant, the size of

Table 10
Economic feasibility calculations.

Plant Metric	Unit	Company name			
		Areej Vegetable Oils & Derivatives	ACWA Power Barka I	Al Ghubra Power & Desalination	Al Rusail Power Plant
Average net power output	kWe	2.46	26.8	29.9	12.1
ORC size, kWe	kWe	5	30	40	20
ORC unit		1			
ORC price [30]	$/kWe	4150	2960	2960	2960
Days per year	day	365			
Hours per year	hr.	8760			
Power factor	%	85			
Capex Inputs					
ORC unit price	USD	20,750	88,800	118,400	59,200
Additional Equipment	USD	3112.5	13,320	17,760	8880
Construction, ancillary construction costs, insurance, etc	USD	2282.5	9768	13,024	6512
O&M expenses, 3% form the unit price	USD	622.5	2664	3552	1776
Total Expenses	USD	26767.5	114,552	152,736	76,368
Generated Electricity					
Generated Electricity	kWh	18317.16	234768.00	261924.00	105996.00
Electricity Tariff	$/kWe	0.078			
Revenue	$/kWe	1428.74	18311.90	20430.07	8267.69
EBITDA		806.24	15647.90	16878.07	6491.69
Rev. %	%	56.43	85.45	82.61	78.52
Payback Period (PBP)		18.74	6.26	7.48	9.24

ORC units that fit to be install at these locations were found to be 30 kWe, 5 kWe, 40 kWe and 20 kWe, respectively. Tocci et al. [30], stated that the specific cost of ORC units should not exceed the value of 3500 €/kW and 2500 €/kW, in the power range of 5–10 kWe and 10–100 kWe, respectively. Accordingly, the cost of ORC unit at each company was calculated as shown in Table 10. In addition to the ORC unit price, the following additional expense were considered:

a) Operating and Maintenance expense (O&M), which is basically including, plant management, labor, maintenance cost, utilities-electricity (purchased power of the parasitic load). 3% from the ORC unit price was used for estimating the O&M expense.
b) Construction, ancillary construction costs, insurance, etc. the following expense fall under this package: mechanical installation, electrical connection, fittings, instrumentations, travel, etc. Lemmens [31], assumed this expense to be 11% of the unit price.
c) Additional equipment, which refers to the water pump of the cooling cycle, cooling tower, shipping cost, etc. It has been assumed to be 15% form the ORC unit price.

For the sake of simplicity, it has been assumed that the ORC plant to operate 85% of the time, which corresponds to 7446 h/year and the inflation rate and escalation have been ignored. The electricity tariff is 0.078 cent/kWh (based on Tariff category of Muscat electricity distribution company). The data of the economic feasibility are listed in Table 10 from which it can been concluded that, installing ORC unit at ACWA Power Barka I seems an attractive project as it payback period is approximately 6 years which is somehow acceptable of ORC technology projects and the percentage of its revenue reached to 85%. The second attractive place for using the ORC unit was found to be at Al Ghubra Power & Desalination, while the worse economic performance found to be at Areej Vegetable Oil & Derivatives. Despite its revenue percentage was about 50%, it payback period is very long almost 19 years.

6. Conclusions

The utilization of the ORC to maximize thermal energy efficiency of the thermal cycle for some selected industries in Oman have been evaluated and analyzed. The main conclusions drawn from this study show that the ORC technology seems to be a practical solution for converting waste heat into power for industries having waste thermal energy sources of higher temperature and mass flow rate. For better performance of the ORC unit, the ratio of the refrigerant mass flow rate to the waste heat source mass flow rate should be 0.35 as an optimum value. However, not only the mass flow rate affected the thermal performance of the ORC unit, the water coolant temperature has a significant influence on the performance, i.e. the higher performance of the ORC unit was achieved on February when the cooling water temperature is at its coolest and sharply decreases during the summer to its minimum in June and July and steadily increases after. In addition, it has been observed that the waste heat source temperature plays a decisive role on the performance of the ORC unit. Based on the average cooling water temperature and optimum dimensionless mass flow rate the values achieved by *ACWA Power Barka I* waste heat source are 29 kW and 7.9% overall thermal efficiency due to its high heat source temperature and flow rate *while Areej Vegetable Oils & Derivatives* achieved 2.9 kW and 4.1% due to its lower heat source temperature and flow rate.

From the economic point of view, using ORC unit as waste heat recovery technique in ACWA Power Barka I was found to be a feasible project in terms of payback period of approximately 6 years and revenue percentage of 85%. In contrast, the available waste heat at Areej Vegetable Oil & Derivatives cannot be economically recovered to electric power as a result of its long time-span of payback period.

CRediT authorship contribution statement

Abdullah Al-Janabi: Project administration, Supervision, Methodology, Validation, Writing - original draft, Writing - review & editing. **Ghassan Al-Hajri:** Data curation, Formal analysis, Investigation, Validation. **Tariq Al-Maashani:** Data curation, Formal analysis, Investigation, Validation.

Declaration of Competing Interest

The authors declare that they have no known competing financial interests or personal relationships that could have appeared to influence the work reported in this paper.

Acknowledgements

The authors would like to thank *ACWA Power Barka I*, *Areej Vegetable Oil & Derivatives*, *Al Ghubra Power & Desalination, Al Rusail Power Plant, and Sharq Sohar Steel Rolling Mills LLC* for supporting our work by providing useful technical data for the available waste heat sources in their industries. The authors also wish to acknowledge the CoolProp for providing the *R-245fa* library for free of charge.

References

[1] Vanslambrouck, B., Vankeirsbilck, I., Paepe, M. De., Gusev, S., 2011, Turn waste heat into electricity using an organic Rankine cycle, 2nd European Conference on Polygeneration. Tarragona, Spain, pp. 1-14.
[2] United States Department of Energy, 2008, Waste Heat Recovery: Technology and Opportunities in U.S. Industry, Industrial Technologies Program.
[3] Natural Resources Canada, 2011, http://canmetenergy.nrcan.gc.ca/industrial-processes/1574.
[4] Energy Management Series for Industry, Commerce, and Institutions: Waste Heat Recovery, Canada Centre for Mineral and Energy Technology, Energy, mines, and Resources Canada, 1986.
[5] Ziviani, D., Beyene, A., Venturini, M., 2012, Development and validation of an advanced simulation model for ORC-based system, ASME 2012 International Mechanical Engineering Congress and Exposition. Houston, Texas, Vol. 6, Energy, Parts A and B, pp. 331-345.
[6] K. O'Rielly, J. Jeswiet, Improving industrial energy efficiency through the implementation of waste heat recovery systems, Trans. Canad. Soc. Mech. Eng. 39 (1) (2015) 125–136.
[7] D. Wei, X. Lu, Z. Lu, J. Gu, Performance analysis and optimization of Organic Rankine Cycle (ORC) for waste heat recovery, Energy Convers. Manage. 48 (4) (2007) 1113–1119.
[8] COWI and Partners LLC, 2008, Study on renewable energy resources in Oman. Muscat: Authority for Electricity Regulation.
[9] B. Liu, K. Chien, C. Wang, Effect of working fluids on organic Rankine cycle for waste heat recovery, Energy 29 (2004) 1207–1217.
[10] C. Huijuan, D.Y. Goswami, E.K. Stefanakos, A review of thermodynamic cycles and working fluids for the conversion of low-grade heat, Renew. Sustain. Energy Rev. 14 (2010) 3059–3067.
[11] S. Quoilin, Sustainable energy conversion through the use of organic Rankine cycles for waste heat recovery and solar applications, PhD thesis, Energy Systems Research Unit Aerospace and Mechanical Engineering Department, 2011.
[12] T.C. Hung, T.Y. Shai, S.K. Wang, A review of organic Rankine cycles (ORCs) for the recovery of low-grade waste heat, J. Energy 22 (7) (1997) 661–667.
[13] H. Chen, D.Y. Goswami, E.K. Stefanakos, A review of thermodynamic cycles and working fluids for the conversion of low-grade heat, Renew. Sustain. Energy Rev. 14 (2010) 3059–3067.
[14] T.C. Hung, Waste heat recovery of organic Rankine cycle using dry fluids, Energy Convers. Manage. 42 (5) (2001) 539–553.
[15] ORCycle: From waste heat to electricity. (2012). http://www.orcycle.be/ index.php/en/orctheorie. Accessed 09 March 2012.
[16] Q. Chen, J. Xu, H. Chen, A new design method for Organic Rankine Cycles with constraint of inlet and outlet heat carrier fluid temperatures coupling with the heat source, Appl. Energy 98 (2012) 562–573.
[17] K.K. Srinivasan, P.J. Mago, S.R. Krishnan, Analysis of exhaust waste heat recovery from a dual fuel low temperature combustion engine using an Organic Rankine Cycle, Energy 35 (6) (2010) 2387–2399.
[18] P.J. Mago, L.M. Chamra, K. Srinivasan, C. Somayaji, An examination of regenerative organic Rankine cycles using dry fluids, Appl. Therm. Eng. 28 (8) (2008) 998–1007.
[19] J. Facão, A.C. Oliveira, Analysis of energetic, design and operational criteria when choosing an adequate working fluid for small ORC systems, in: ASME 2009 International Mechanical Engineering Congress & Exposition, Lake Buena Vista, Florida, 2009, pp. 13–19.
[20] US Environmental Protection Agency, Global Warming Potentials of ODS Substitutes, USEPA, Washington DC, 2011.
[21] Secretariat, U. N. E. P. O., 2006, Handbook for the Montreal protocol on substances that deplete the ozone layer, UNEP/Earthprint.
[22] US Environmental Protection Agency, Ozone Layer Protection Glossary, USEPA, Washington DC, 2010.
[23] Facão, J., Palmero-Marrero, A., Oliveira, A. C., 2008, Analysis of a solar assisted micro-cogeneration https://www.seatemperature.org/middle-east/oman/muscat.htm.
[24] G. Zyhowski, A. Brown, Low global warming fluids for replacement of HFC-245fa and HFC-134a in ORC applications, Honeywell, New York, 2015.
[25] V. Maizza, A. Maizza, Working fluids in non-steady flows for waste energy recovery systems, Appl. Therm. Eng. 16 (1996) 579–590.
[26] K. Rahbar, S. Mahmoud, R.K. Al-Dadah, N. Moazami, S.A. Mirhadizadeh, Review of Organic Rankine Cycle for small-scale applications, Energy Convers. Manage. 134 (2017) 135–155.
[27] S. Baral, C.K. Kim, Thermodynamic modeling of the solar Organic Rankine Cycle with selected organic working fluids for cogeneration, Distrib. Gener. Alternative Energy J. 29 (2014) 7–34.
[28] A.S. Panesar, A study of organic Rankine cycle systems with the expansion, master thesis, School Eng. Math. Sci. (2012).
[29] Y.A. Cengel, M.A. Boles, Thermodynamics An Engineering Approach, 8th ed., McGraw Hill Education, New York, 2015.
[30] L. Tocci, T. Pal, I. Pesmazoglou, B. Franchetti, Small Scale Organic Rankine Cycle (ORC): a techno-economic review, Energies 10 (2017) 413.
[31] S. Lemmens, Cost engineering techniques and their applicability for cost estimation of organic rankine cycle systems, Energies 9 (2016) 485.